Universität Potsdam

Arkady Pikovsky, Ulrike Feudel

Characterizing strange nonchaotic attractors

Characterizing Strange Nonchaotic Attractors

Arkady S. PIKOVSKY and Ulrike FEUDEL

Max–Planck–Arbeitsgruppe "Nichtlineare Dynamik",
Universität Potsdam, Am Neuen Palais,
PF 601553, D-14415 Potsdam, Germany.

Abstract

Strange nonchaotic attractors typically appear in quasiperiodically driven nonlinear systems. Two methods of their characterization are proposed. The first one is based on the bifurcation analysis of the systems, resulting from periodic approximations of the quasiperiodic forcing. Secondly, we propose to characterize their strangeness by calculating a phase sensitivity exponent, that measures the sensitivity with respect to changes of the phase of the external force. It is shown, that phase sensitivity appears if there is a non-zero probability for positive local Lyapunov exponents to occur.

1   Introduction

Strange objects are not very rare in science. A well-known example is a strange attractor – an object in a phase space of a nonlinear dynamical system, that usually corresponds to chaotic behavior of the system. Approximately ten years ago Grebogi, Ott, Pelikan and Yorke [1] showed that in nonlinear dynamical systems strange nonchaotic attractors can exist. These objects mainly appear in quasiperiodically forced nonlinear systems and have since that time been observed, e. g., in [2, 3, 4, 5, 6, 7, 8]. Although SNAs seem to have rather unusual properties, it was shown in refs.[2, 4] that they are typical in the sense that they occur on a set of positive measure in the parameter space. SNAs have been observed in different dynamical systems, including the quasiperiodically forced circle map[2] and the damped pendulum[9], they have been also related to the properties of the Schrödinger equation with a quasiperiodic potential[10]. Nevertheless, the theory of strange nonchaotic attractors (SNAs) is much less developed then the theory of strange attractors. In particular, for strange attractors we know typical routes of their appearance (period doubling, intermittency, etc.) and disappearance (e. g., crisis) [11, 12]. Statistical properties of chaotic attractors are also well studied. In

1

contrast to that the way how SNAs arise, and what are their statistical characteristics, remain still as not completely solved questions. One particular route to strange nonchaotic attractor has been recently discussed by Heagy and Hammel [13].

A strange nonchaotic attractor was defined in ref.[1] as an attractor which is not a finite set of points and is not picewise differentiable, and for which typical orbits have a negative Lyapunov exponent. Thus, in order to establish that a SNA is really observed, one has: (1) to calculate the Lyapunov exponent and (2) to check that the attractor is not differentiable. The first task is relatively simple, because there are reliable methods for calculating the Lyapunov exponent, and if it is negative, then one can be sure that the attractor is nonchaotic. The second task is much more difficult. In the case of some ideal attractors the nondifferentiability can be proved analytically (see [1] and the discussion below), but often the absence of differentiability is argued only basing on the pictures of attractors.

It is the aim of the present investigation to look at the difference between non-strange attractors and SNAs more carefully. We suggest several approaches, which enable one to distinguish between SNA and non–strange (but looking very similar to strange) nonchaotic attractors, and apply these methods to some of the previously studied systems. Mainly we shall deal with the basic model, introduced in [1], we shall describe it in Section 2. The first approach (Section 3) is based on the observation that any irrational number can be appoximated by an infinite number of rationals. Thus, using such an approximation we construct a sequence of periodically forced systems and study their bifurcation phenomena, in order to determine the structure of the attractor of the limiting quasiperiodically forced system. Another approach (Section 4)is based on the analysis of sensitivity of the attractor to the phase of the external force. While sensitivity to initial conditions leads to the notion of the Lyapunov exponent, we will characterize the sensitivity to external force by a *phase sensitivity exponent*, which will allow to distinguish strange and non-strange attractors. We will also show that the phase sensitivity exponent is closely connected to the properties of the distribution of local Lyapunov exponents. This helps to explain, why the transition to chaos in quasiperiodically forced systems usually occurs through SNA. We will also discuss, how this exponent can be calculated directly from observed time series of a system.

2 The basic model

Let us start with the system, for which the SNA has been first reported[1]. It is the two–dimensional map

$$x_{n+1} = f(x_n, \theta_n) = 2\sigma(\tanh x_n)\cos(2\pi\theta_n), \tag{1}$$

$$\theta_{n+1} = \theta_n + \omega \mod 1. \tag{2}$$

where $f(x, \theta) = f(x, \theta + 1)$. In fact, Eq. (1) describes a forced nonlinear system. If ω is rational, the forcing is periodic, while for irrational ω the forcing is quasiperiodic.

A SNA may be observed only in the case of quasiperiodic forcing. In ref.[1] ω was set to be the reciprocal of the golden mean: $\omega = (\sqrt{5} - 1)/2$. It was analytically shown in ref.[1] that a SNA in system (1) – (2) exists for $|\sigma| > 1$. The proof consists of two steps. Firstly, one can see that for typical trajectories of (2) the trivial state $x = 0$ is unstable and some non-zero x is observed. Secondly, there are exceptional trajectories of (2) passing exactly through $\theta = \frac{1}{4}$ and $\theta = \frac{3}{4}$ (where $\cos(2\pi\theta) = 0$) and therefore x is equal to zero for all n. Since all trajectories of (2) are dense on the interval $[0, 1)$, the resulting attractor is discontinuous and not differentiable in a dense set of points (Fig. 1a).

Moreover, the robustness of the occurrence of SNAs with respect to small pertur-bations of system (1,2) has been checked in [1] by adding a further term in Eq. (1). The first equation of the map reads now

$$x_{n+1} \quad = \quad f(x_n, \theta_n) = 2\sigma(\tanh x_n)\cos(2\pi\theta_n) + \alpha\cos(2\pi(\theta_n + \beta)) \qquad (3)$$

where α and β are additional parameters. In the case $\alpha \neq 0$ it is difficult to decide, basing only on the numerical picture (Fig.1b) whether the attractor is strange or not. We will be able to distinguish strange and nonstrange case basing on the presented below methods.

3   Rational Approximations and their Bifurcations

Our first approach in investigating system (1) – (3) is based on the approximation of the irrational value of ω with rationals. This approach is well-known in studies of phase–locking phenomena in Hamiltonian (KAM theory)[14, 15] and dissipative (transition to chaos through quasiperiodicity) [16, 17] systems. For the golden mean irrational the adjusting rationals can be obtained from the continued fraction rep-resentation of ω, they have the form $\omega_k = F_{k-1}/F_k$, where $F_k = 1, 1, 2, 3, 5, 8, \ldots$ are the Fibonacci numbers. The irrational rotation number turns out to be the limit: $\omega = \lim_{k\to\infty} \omega_k$. Using this approximation we study instead of system(1) – (3) the behaviour of an infinite set of systems where the irrational frequency ω is replaced by its rational approximate ω_k. If we analyze these systems for every k then we expect that the properties of system (1) – (3) can be obtained by taking the limit $k \to \infty$. Thus let us consider Eqs. (1) and (3) together with

$$\theta_{n+1} = \theta_n + \omega_k \qquad \text{mod } 1. \qquad (4)$$

The trajectory of the map (4) consists of F_k points uniformly distributed on the interval $[0, 1)$. Now Eq. (1) is a periodically (with period F_k) forced nonlinear map. Or, if we consider only each F_k-th point (some kind of Poincaré map), then the system is governed by an autonomous nonlinear map. This map is smooth and may have one stable fixed point, or several stable fixed points together with unstable
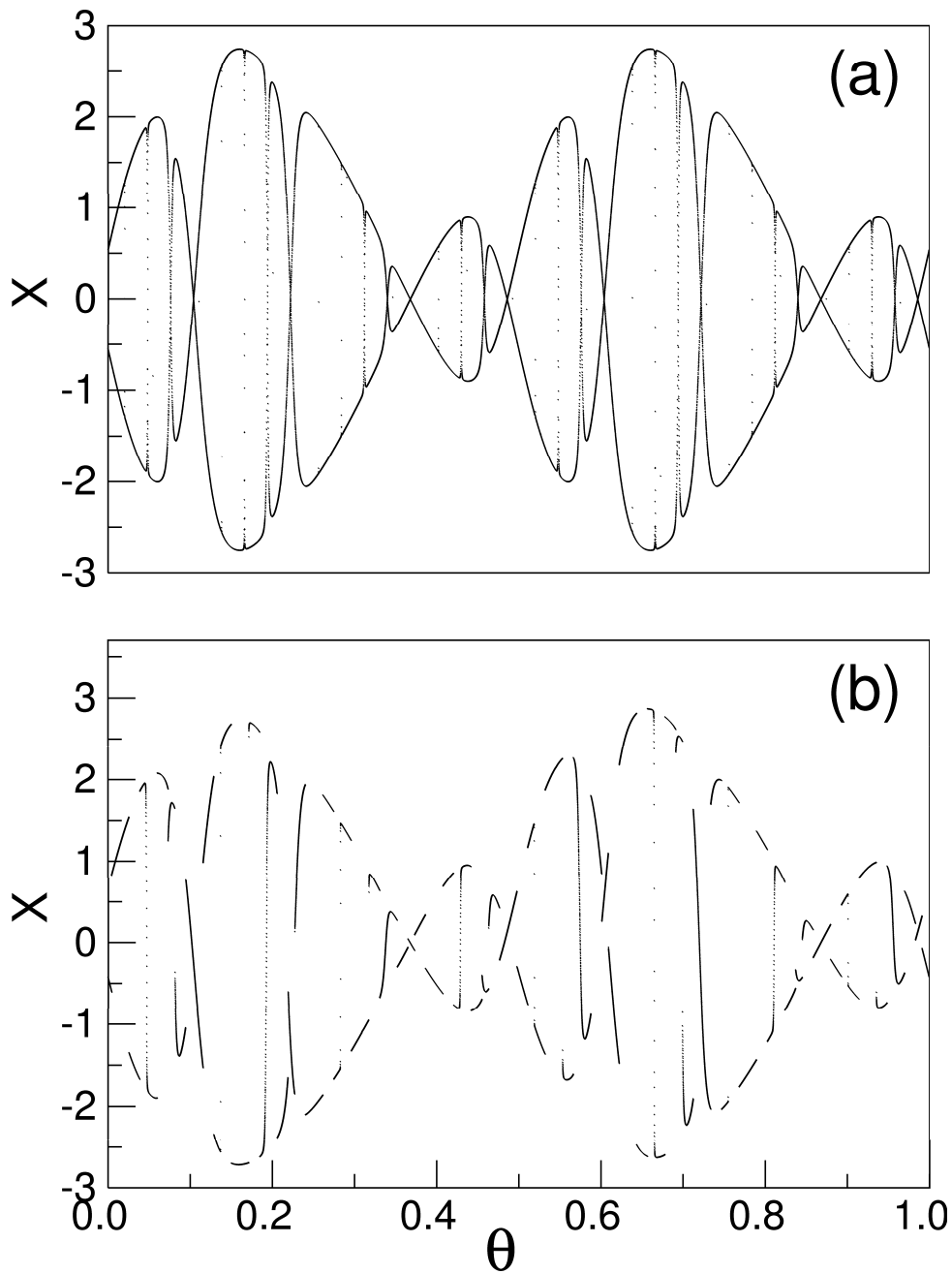
3

Figure 1: (a) Phase portrait of SNA in the system (1,2) for $\sigma = 1.5$;
(b) Phase portrait of a nonstrange attractor in the system (2,3) for $\sigma = 1.5$, $\alpha = 0.2$, $\beta = 1/8$.

ones, or stable periodic orbits, or even a strange attractor. The last possibility is, however, excluded for the particular choice of the nonlinear function (3). The attracting set in system (1),(3) and (4) depends on the parameters σ, α, β, and, what is very important, on the initial phase θ_0 in Eq. (4). We call this value θ_0 *phase shift*. It is clear, that it is sufficient to change θ_0 in the interval $[0, 1/F_k)$ in order to get all possible attracting sets in system (1),(3),(4), because in this case the set of all θ values fills the whole interval $[0, 1)$. Changing θ_0 continuously in the whole interval $[0, 1/F_k)$ and drawing the attracting set on the (x, θ) plane for each of the chosen initial phases θ_0, we get the k–th approximation of the attractor in system (1) – (3) as the union of all occurring attracting sets. Investigating these approximations, we can classify the properties of the limiting attractor.

Because we are interested in distinguishing between strange and nonstrange attractors, smoothness properties of the attracting set in the limit $k \to \infty$ are important. Generally, there are 3 possibilities:
(A) The approximating attracting set is nonsmooth for sufficiently large k.
(B) The approximating attracting set is smooth for any k–th rational approximation, but the maximum derivative
$\max\{dx_\sigma/d\theta : \quad 0 \leq \theta < 1, \ \sigma \in$ all branches of the attracting set$\}$ grows indefinitely with k, so that the limiting set cannot be considered as a smooth one.
(C) The approximating attracting set is smooth for all large k and the maximum derivative is bounded from above.
In the following we use this classification to show that the cases (A) and (B) correspond to a SNA, while case (C) gives a non–strange attractor.

For system (1) – (3) with ($\alpha = 0, |\sigma| > 1$) the existence of SNA was proven in ref.[1]. We have constructed the attracting set for different rational approximations and found, that it exhibits bifurcations as the parameter θ_0 changes (see Fig. 2). For those values of θ_0, for which one of the θ_n is very close to $\frac{1}{4}$ (where $\cos(2\pi\theta) = 0$) there is only one stable fixed point $x = 0$, while for other values of θ_0 either a pair of stable fixed points or a symmetric period–2 cycle exists. Note, that in the bifurcation points observed here the derivative of one branch of attracting sets with respect to θ_0 is infinite. All occurring bifurcation points are of that type that the tangent of one branch of attracting sets is orthogonal to the θ_0 axis (turning points, pitchfork bifurcations and period doublings). This picture of bifurcations is qualitatively the same for all k which has been checked for periods up to $F_k = 987$. Furthermore, the considered interval $0 \leq \theta_0 < 1/F_k$ gets smaller and smaller with increasing k so that the total number of bifurcation points for $\theta \in [0, 1)$ increases. In the limit $k \to \infty$ there are infinitely many bifurcation points with infinite derivative with respect to θ_0 and therefore, we conclude that the limiting attractor is strange corresponding to case A. Because for all k only nonchaotic attractors exist in system (1),(3),(4), we conclude that the limiting attractor is nonchaotic.

Basing on this picture, we may consider the existence of bifurcations (when the phase shift is considered as a parameter) in the rational approximations as sufficient condition for strangeness of the limiting attractor.
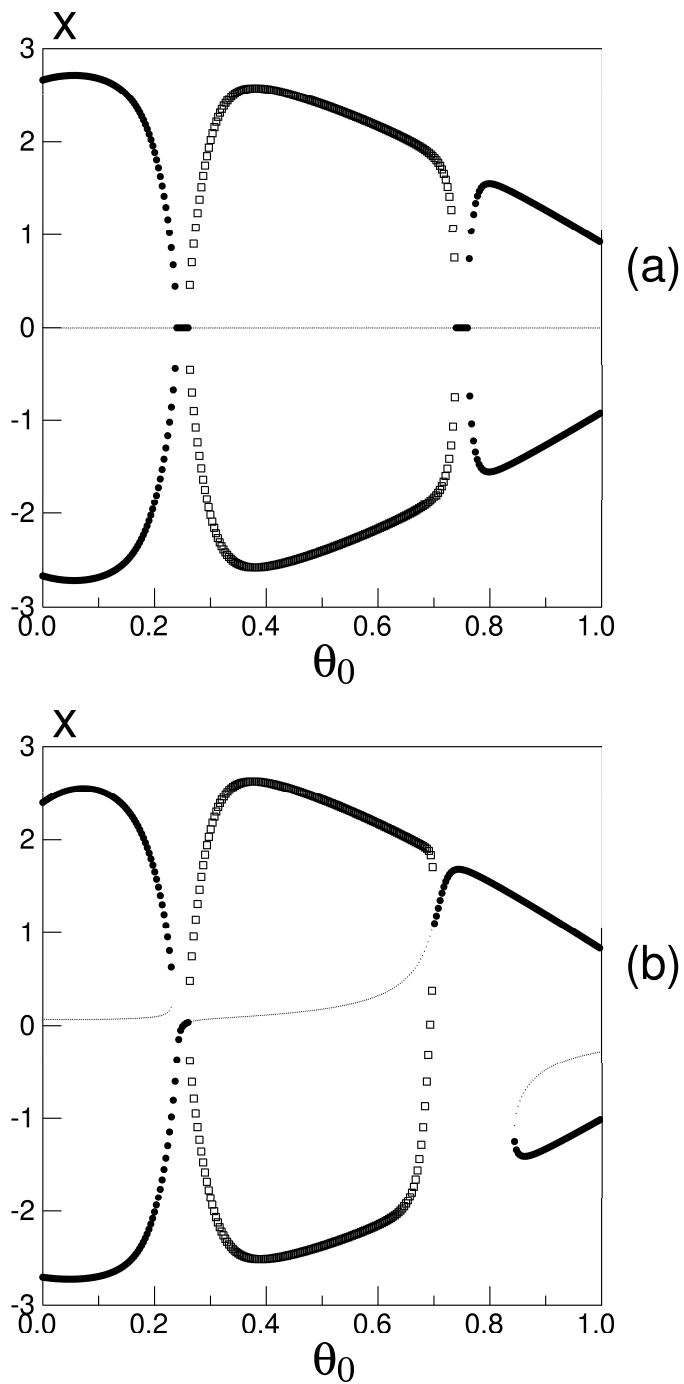
5

Figure 2: Attracting set for the approximation with period $F_k = 5$: (a) $\alpha = 0$, (b) $\alpha = 0.2$. Dots - unstable fixed points, filled circles - stable fixed points, open squares - period–2 orbits.

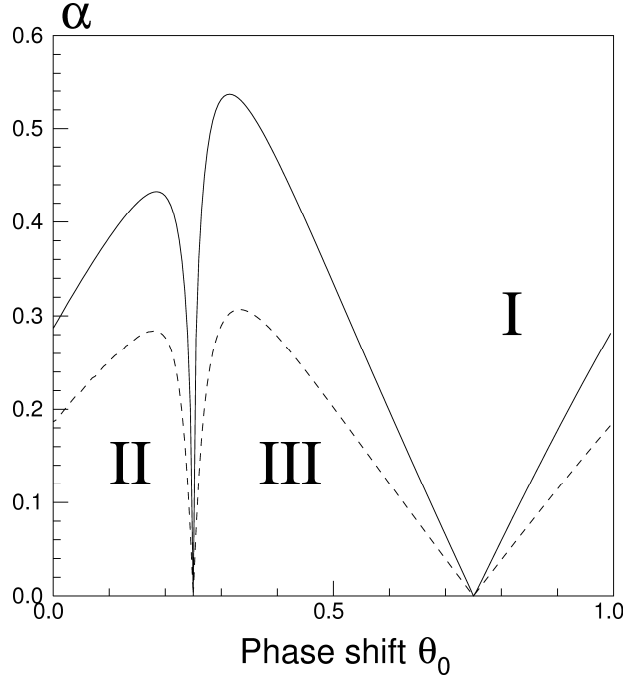The phase shift $\theta_0 \in [0, 1/F_k)$ is shown normalized to its maximum value $1/F_k$.

Figure 3: Bifurcation diagram on the (α, θ_0) plane; solid line : $F_k = 13$, dashed line: $F_k = 21$. In the region I there is only one stable fixed point; in the region II there are two stable fixed points and an unstable one; in the region III there is one unstable fixed point and a stable period-2 cycle.

Let us now consider system (1) – (3) with $\alpha \neq 0$. (The parameters $\beta = 0.125$ and $\sigma = 1.5$ are fixed). Fig. 3 shows bifurcations sets in the (θ_0, α) plane for two different k values. We see that the interval of α values $-\alpha_{max} \leq \alpha \leq \alpha_{max}$, for which bifurcations occur, decreases with increasing k. Fig. 4 shows that $\alpha_{max} \sim F_k^{-1}$. Thus we conclude, that for a fixed $\alpha \neq 0$ there are no bifurcations in the rational approximations for sufficiently large k, and therefore the system is of type A only for $\alpha = 0$. To distinguish between the cases B and C, we have calculated the maximum value of the derivative $dx/d\theta$. A typical picture of approximating attracting set is shown in Fig. 5 which indeed seems to have infinite derivative. However, when we calculate $\max\{|dx/d\theta| : \quad 0 \leq \theta < 1\}$ for the graph Fig. 5, we get a value that *does not increase with increasing* k (see Fig. 6)!

This means that the attractor here is of type C and the limiting attracting set is not discontinuous. The maximum value of derivative depends on α (see Fig. 6) and grows as α decreases. The attractor becomes more and more close to a differentiable one as α decreases, but a SNA exists only for $\alpha = 0$.

Additionally, we considered another system, for which a strange nonchaotic attractor

7

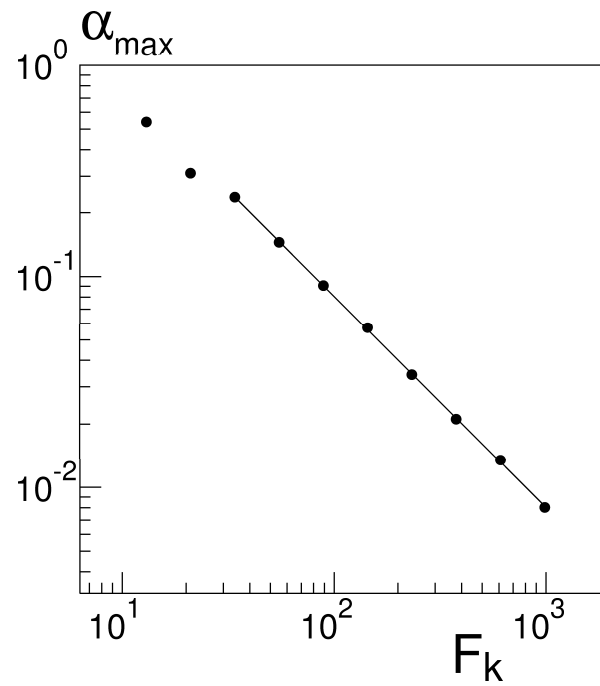Figure 4: Maximum value of α, for which bifurcations occur, vs. approximation period. The best fitting line has the slope -1.
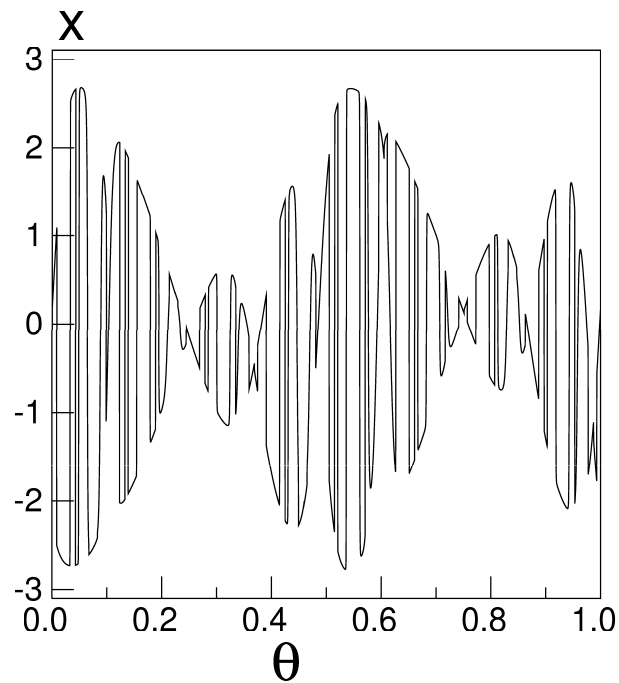

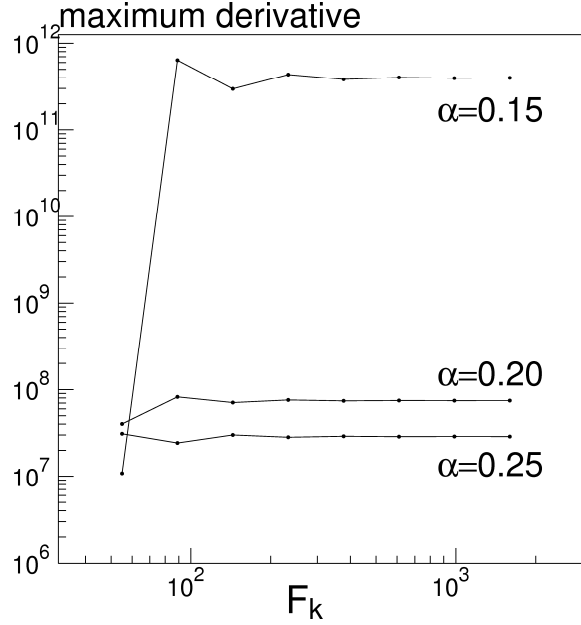Figure 5: Approximation of the attracting set with $F_k = 233$ for $\alpha = 0.2$.

8

Figure 6: Maximum derivative of the graph Fig. 5 vs. approximation period, for different α values.

was reported [2],[3],[5], namely the quasiperiodically forced circle map

$$x_{n+1} = x_n + K + \frac{V}{2\pi}\sin 2\pi x_n + \frac{C}{2\pi}cos 2\pi\theta_n \qquad \mathrm{mod}\ 1, \qquad (5)$$

$$\theta_{n+1} = \theta_n + \omega \qquad \mathrm{mod}\ 1. \qquad (6)$$

We fixed $K = 0.2841$ and $V = 0.95$ as in [3], and varied C in a parameter range where the maximum Lyapunov exponent is always negative. We obtained, that bifurcations of the approximating attracting sets appear only at some critical value $C_{cr}^{(k)}$, depending on k (see Table 1). For large k variations of $C_{cr}^{(k)}$ are rather small and $C_{cr}^{(\infty)} \approx 1.1303$ appears to be the point of transition from non–strange to strange nonchaotic attractor (Fig.7).

Table 1.

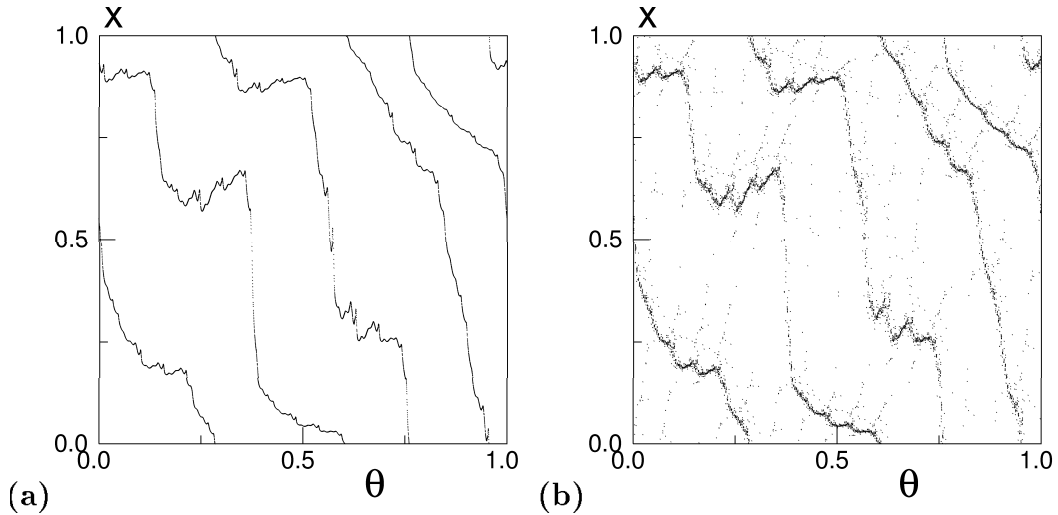| Period of rational approximation	C_{cr}
377	1.130093
610	1.130401
987	1.130284
1597	1.130305
2584	1.130299
4181	1.130365
6765	1.130301

9

Figure 7: Nonstrange and strange attractors for the system (5,6) near the transition point: (a) $C = 1.1302$ (b) $C = 1.1304$.

It is worth noting that the bifurcation diagram for this system is rather complicated. In particular, for some values $C > C_{cr}^{(\infty)}$ no bifurcations are observed, and in these cases the limiting attracting set appears also to be non–strange.

Basing on the presented results, we may formulate the hypothesis, that a strange nonchaotic attractor exists only in the case where rational approximations possesses bifurcations for sufficiently large k. This allows one to formulate a relatively simple method of detecting SNA, using rational approximations of the irrational external frequency and looking for bifurcations as the phase shift changes. The existence of bifurcations means that the attractor is strange, if there are no bifurcations; then the attractor is nonstrange. This method is relatively simple to perform, and seems to be applicable in real experiments as well.

4 Phase sensitivity properties

4.1 Phase sensitivity exponent

As outlined in the previous section the consideration of the maximum derivative $\partial x / \partial \theta$ provides a suitable tool to distinguish between stange and nonstrange attractors. Next, we want to calculate this derivative not for the approximations but for the attractor of the quasiperiodically forced system itself. Let us first characterize the smooth attractor in Fig. 1b. This attractor is given by a curve $x = F(\theta)$, and we want to calculate the derivative $\partial x / \partial \theta$. This derivative changes along a trajectory

10

$(x_0, \theta_0), (x_1, \theta_1), \ldots$ According to eq. (2), $\partial x_m / \partial \theta_m = \partial x_m / \partial \theta_k = \partial x_m / \partial \theta_0$ for any m, k. Therefore, we will omit the index of θ and call it "derivative with respect to the external phase". From eq.(1) we easily get a recurrence relation

$$\frac{\partial x_{n+1}}{\partial \theta} = f_\theta(x_n, \theta_n) + f_x(x_n, \theta_n)\frac{\partial x_n}{\partial \theta}, \tag{7}$$

so starting from the correct initial derivative $\partial x_0 / \partial \theta$ we get derivatives at all points of the trajectory:

$$\frac{\partial x_N}{\partial \theta} = \sum_{k=1}^{N} f_\theta(x_{k-1}, \theta_{k-1}) R_{N-k}(x_k, \theta_k) + R_N(x_0, \theta_0)\frac{\partial x_0}{\partial \theta} \tag{8}$$

where

$$R_M(x_m, \theta_m) = \prod_{i=0}^{M-1} f_x(x_{m+i}, \theta_{m+i}) \tag{9}$$

and $R_0 = 1$. For large n the values of R_n can be represented through the Lyapunov exponent

$$\lambda = <\log|f_x|> \tag{10}$$

as

$$R_n \simeq \pm \exp(\lambda n).$$

Because we consider nonchaotic attractors, the Lyapunov exponent λ is negative and R_n is exponentially small for large n. This means that the derivative does not depend on the initial guess $\partial x_0 / \partial \theta$, and starting iterations of (7) from any initial value (e.g., from zero) we get for large N the correct value of the derivative:

$$\frac{\partial x_N}{\partial \theta} \approx S_N \equiv \sum_{k=1}^{N} f_\theta(x_{k-1}, \theta_{k-1}) R_{N-k}(x_k, \theta_k). \tag{11}$$

This gives a simple procedure for calculating simultaneously the attractor and its derivative with respect to the external phase in the smooth case: one iterates (1), (2) and (7) starting from arbitrary values of x and $\partial x / \partial \theta$, and for large n they converge to the attractor and its derivative, respectively. The partial sums S_N computed by (11) are *bounded* by the maximum derivative $\partial x / \partial \theta$ along the attractor.

In the case of SNA the attractor is nonsmooth and the derivative $\partial x / \partial \theta$ does not exist, so the consideration above is no more valid. But we will use it to show that the assumption of a finite derivative leads in the case of SNA to a contradiction. Let us calculate the partial sums S_N (11), using the same recurrence relations. The results of such calculation for a randomly chosen trajectory are presented in Fig. 8a.

The behavior of the sums seems very intermittent. The key observation is that these sums are *unbounded*. This can be explicitly seen in Fig. 8b, where we plot a maximum

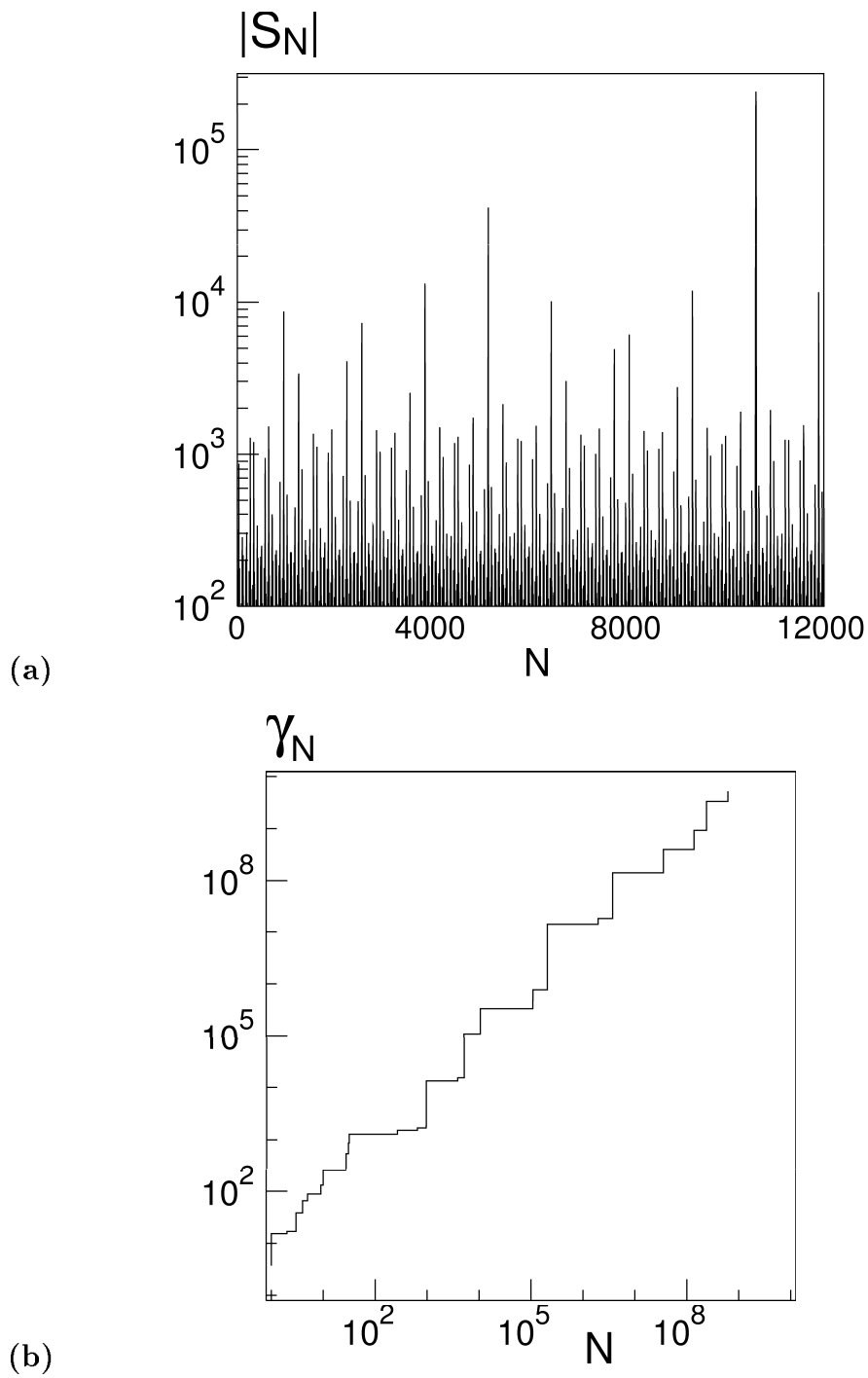$$\gamma_N(x, \theta) = \max_{0 \leq n \leq N} |S_N|. \tag{12}$$

(a)

(b)

Figure 8: Partial sums $|S_N|$ (a) and their maximum γ_N (b) for a trajectory on the SNA shown in Fig.1.
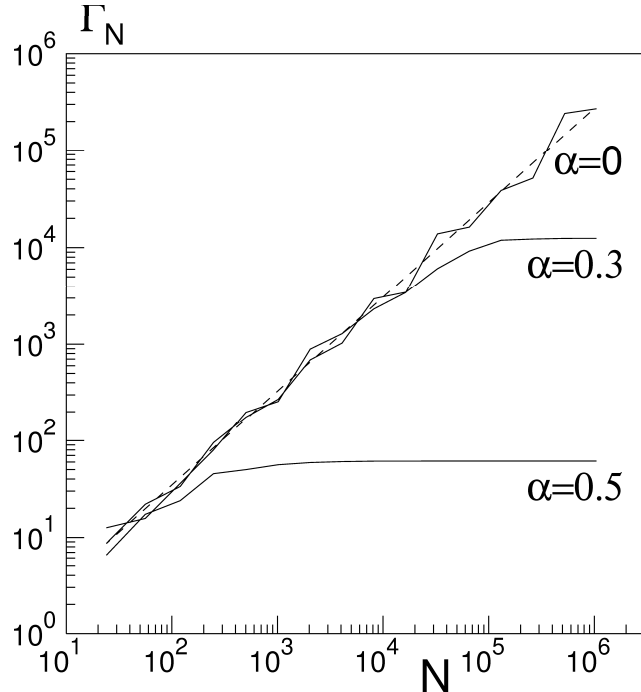
Figure 9: Values of Γ_N vs. N for the system (2,3) for $\sigma = 1.5$, $\beta = 1/8$, different α and 1000 randomly chosen initial conditions. Only at $\alpha = 0$ the dependence may be fitted by a line (dashed line) with slope $\mu \approx 0.97$.

The value of γ_N grows with N, which means that arbitrary large values of $|S_N|$ appear. From this follows immediately that the attractor cannot have finite derivative with respect to the external phase, i.e., the attractor is nonsmooth. Indeed, the assumption of a finite derivative is inconsistent with relation (8), where the second term in the r.h.s. is exponentially small and the first term in the r.h.s. can be arbitrary large. Thus, calculating partial sums (11) (by means of the recurrence relation (7) starting from $\partial x_0 / \partial \theta = 0$), we can distinguish strange (sums are unbounded) and non-strange (sums are bounded) attractors.

The growth rate of the partial sums with time represents a degree of strangeness of the attractor, and can be used as a quantitative characteristics of SNAs. For this purpose we need a quantity that is independent of a particular trajectory, but represents average properties of the attractor. The appropriate quantity seems to be the minimum value of $\gamma_N(x, \theta)$ with respect to randomly chosen initial points (x, θ):

$$\Gamma_N = \min_{x, \theta} \gamma_N(x, \theta), \tag{13}$$

presented in Fig.9.

We would like to mention that while other quantities which do not depend on a particular trajectory may be defined (e.g., the average of $\gamma_N(x, \theta)$), the minimum

value allows a more reliable inference that the attractor is non-smooth. Moreover, its numerical convergence is very good, so that it is enough to take about 1000 randomly chosen initial conditions (x, θ). From Fig.9 we see that Γ_N grows with N as

$$\Gamma_N \simeq N^\mu \qquad (14)$$

where the value $\mu \approx 0.97$ is a quantitative characteristics of the strangeness of the attractor, we call it *phase sensitivity exponent*. A rough theoretical estimation of the exponent μ based on the distribution of local Lyapunov exponents will be given in the next section.

The calculation of the phase sensitivity exponent allows one to distinguish between strange and nonstrange attractors. In Fig.9 we present results of the calculations for different values of the parameter α in Eq.(3) (parameter $\beta = 1/8$ was fixed like in [1]). One can see that for $\alpha = 0.5$ and $\alpha = 0.3$ the value of Γ_N saturates with N, so the phase sensitivity exponent is zero. This confirms the results of section 2, where it was shown that a SNA in system (2,3) exists only for $\alpha = 0$ (which corresponds to system (1,2)).

4.2 Local Lyapunov exponents

Here we discuss the relation between the phase sensitivity exponent and the usual maximum Lyapunov exponent which reflects the sensitivity to the initial conditions. Let us first analyze the dynamics of the partial sums, shown in Fig. 8, in more detail. It is seen that the behavior of the partial sums is very intermittent: during large time intervals the values of $\hat{S}_N$ are relatively small, while there are short but extremely high peaks. One of these peaks is enlarged in Fig.10a.

During the peak the partial sum grows approximately exponentially in time, and then returns to a small value. Let us compare this behavior with the representation of the partial sum Eq.(11). Because the derivatives f_θ are bounded, the sum can be large only if one of the factors R is large. As it follows from the definition (9), the factor R is a local multiplier that determines local (in phase space) sensitivity of the motion. The corresponding local Lyapunov exponent is defined as [18, 19, 20]

$$\Lambda_M(x, \theta) = \frac{1}{M} \log |R_M(x, \theta)| \qquad (15)$$

and the usual Lyapunov exponent (10) is the limit: $\lambda = \lim_{M \to \infty} \Lambda_M$. Thus, we conclude that high bursts of the finite sum correspond to such parts of the trajectory possessing a positive local Lyapunov exponent. This can be explicitly seen in Fig. 10b, where instantaneous growth rates Λ_1 (defined by Eq. (15) with $M = 1$) in the burst region are presented. During approximately 25 iterations, Λ_1 is mostly positive, and this produces a large partial sum.

Properties of local (in phase space) Lyapunov exponents have been widely discussed for chaotic systems [21, 22]. Based on central-limit-theorem-like arguments [22] one
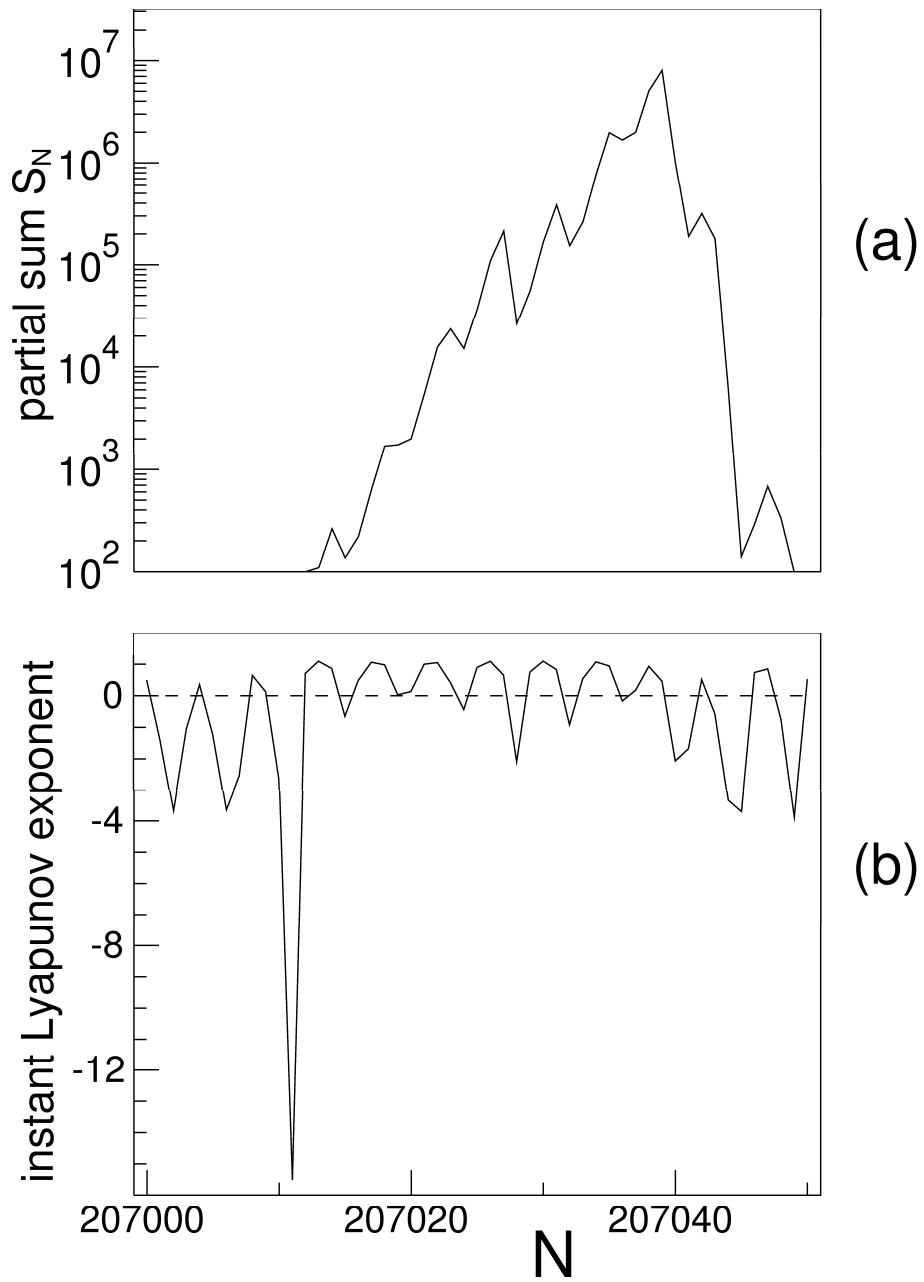
Figure 10: Enlarged burst of the partial sum $|S_N|$ presented in Fig.8 (a) and corresponding instantaneous Lyapunov exponents (b).

can expect, that for large M the distribution density of the exponents scales (in the leading exponential order) as:

$$W_M(\Lambda) \sim \exp(M\phi(\Lambda)) \tag{16}$$

The scaling function $\phi(\Lambda)$ is convex and has a maximum exactly at $\Lambda = \lambda$[18, 19]. Usually, this function is defined on a finite interval: $\phi(\Lambda) > -\infty$ for $\Lambda_{\min} \leq \Lambda \leq \Lambda_{\max}$ (the quantities $\Lambda_{\min}$ and $\Lambda_{\max}$ correspond to minimum and maximum local expansion rates on the chaotic set). In the case of SNA scaling properties of local Lyapunov exponents are not known. We assume here, that relation (16) is still valid. One argument for this assumption is that the power spectrum of SNAs is very dense and close to a broad-band one [2, 4] . This corresponds to an effective decay of correlations, which allows one to apply the same arguments as for chaotic systems. On the other hand, scaling (16) does not contradict the numerics presented below.

Now, we can describe SNAs in terms of local Lyapunov exponents: a SNA appears when the scaling function $\phi(\Lambda)$ has a maximum at negative Λ, but has finite values also for positive Λ: $\Lambda_{\max} > 0$. The first property ensures that the attractor is nonchaotic. From the second property it follows that the attractor is non-smooth. Indeed, in this case the local Lyapunov exponent can be positive with non-zero probability. For such pieces of a trajectory the local multiplier $R_M(x, \theta) = \exp(M\Lambda_M(x, \theta))$ can be arbitrary large according to relation (15), hence, the partial sum (11) can be arbitrary large, and this means nonexistence of derivative with respect to the external phase. Thus, the existence of a positive $\Lambda_{\max}$ for the scaling function (16) in the limit $M \to \infty$ means that the attractor is strange.

We computed the distribution function $W_M(\Lambda)$ for system (1,2) (see Fig. 11). Since positive Λ are of most interest, only this part of the distribution is presented. If the scaling (16) holds, distributions for different M must have the same form. This is only approximately true for the largest values $M = 45$ and $M = 50$ for which we could obtain enough statistics. It is also worth mentioning that the value $\Lambda_{\max}$ is remarkably stable for all $M \leq 50$: $\Lambda_{\max} \approx 0.45$. This value can be also estimated analytically. Indeed, as shown in ref.[1], an orbit $x \equiv 0$ with a Lyapunov exponent $h = \log|\sigma|$ belongs to the attractor. Thus, for $\sigma = 1.5$ we can estimate $\Lambda_{\max} \geq \log|\sigma| \approx 0.405$. We can also roughly estimate the form of the function $\phi(\Lambda)$ for positive Λ. Suppose that only those pieces of orbits that start near $x = 0$, i.e. near $\theta = \pi/4$, $3\pi/4$ contribute to positive Λ. The orbit starting at a point $x_0 \approx 0$ spends $T \leq M$ iterations in the vicinity of line $x = 0$, where we can estimate T as $T \approx -\log|x_0|/h$. During these iterations the local Lyapunov exponent achieves the value $\Lambda(x_0) \approx hT/M = -\log|x_0|/M$. If we assume that the values of x_0 are distributed uniformly (this follows from uniform distribution of phases θ, see Fig. 1) and take into account that the local Lyapunov exponent cannot be larger than h (if the orbit does not leave the vicinity of line $x = 0$ during M iterations), we get a "truncated Poissonian distribution" of positive local Lyapunov exponents

$$W_M(\Lambda) \sim \begin{cases} M\exp(-M\Lambda) & \text{if } \Lambda < h, \\ \exp(-Mh)\delta(\Lambda - h) & \text{if } \Lambda \geq h. \end{cases} \tag{17}$$
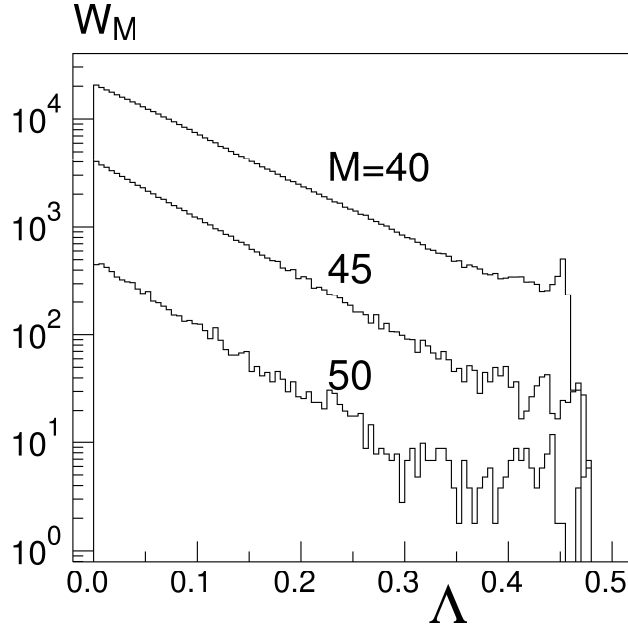
16

Figure 11: Histograms of positive local Lyapunov exponents of the SNA shown in Fig.1a.

This simple estimate qualitatively fits the numerically obtained histograms Fig.11. Note also that it has the scaling form (16).

Using the knowledge about the distribution of local Lyapunov exponents, we can estimate the phase sensitivity exponent μ introduced in the previous section. During time N only events with a probability larger then $1/N$ may be expected to occur. Thus, the largest Lyapunov exponent Λ_{max} may be observed only for time intervals M satisfying $W_M(\Lambda_{max}) \sim 1/N$. Taking into account (17), we get $M \sim h^{-1} \log N$, and the maximum local multiplier that may be observed during time N is then $R \sim \exp(hM) \sim N$. Supposing that the partial sum is dominated by the term with the largest multiplier, we finally obtain $\Gamma_N \sim N$, which means that $\mu = 1$. This estimation for the phase sensitivity exponent fits rather good the data presented in Fig. 9.

4.3   Sensitivity from time series

In this section we discuss how the phase sensitivity can be estimated from an observed time series of a SNA. Suppose we know an orbit (x_n, θ_n) in the two-dimensional (x, θ)-space. Let us notice first that because θ is quasiperiodic, for each given small ε one can find such a n_0 that the distance $\varepsilon_0 = |\theta_{n_0} - \theta_0| < \varepsilon$. Then the quantities $|(x_{k+n_0} - x_k)/(\theta_{k+n_0} - \theta_k)| \equiv |(x_{k+n_0} - x_k)/\varepsilon_0|$ give estimates of the derivative $\partial x/\partial \theta$ along the orbit. If we construct from our orbit (x_n, θ_n) "two"
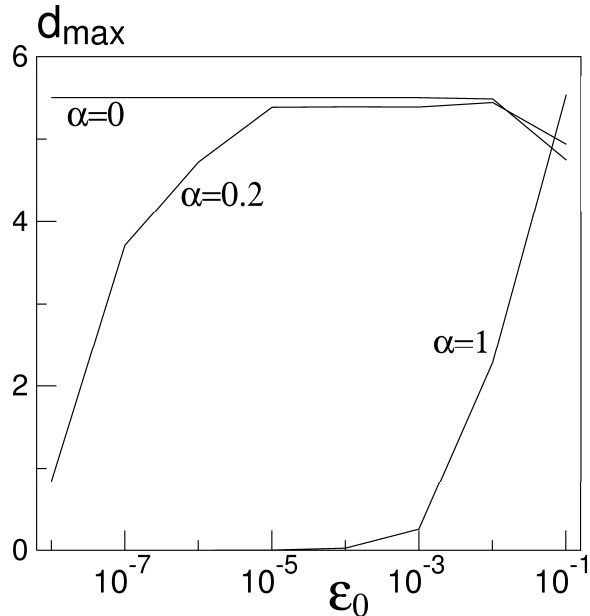
17

Figure 12: Maximum distance d_{max} vs. ε_0 for different values of α; the maximum number of iterations was $N \approx 6 \cdot 10^{11}$ for $\alpha = 0$ and 0.2 and the smallest ε_0.

orbits starting with (x_0, θ_0) and (x_{n_0}, θ_{n_0}) then the phase difference $|\theta_{k+n_0} - \theta_k|$ remains constant during the whole time evolution. The difference between the two trajectories is only determined by the difference $|x_{k+n_0} - x_k|$. This difference can be used as a measure to check smoothness properties of an attractor. If we suppose that the attractor is discontinuous then we expect that the distance between the two trajectories exhibits a complicate time behavior with several peaks similar to the time evolution of $\partial x/\partial \theta$ (Fig.8). Indeed, we have obtained in the case of a strange non-chaotic attractor in system (1,2) such a complex variation of the distance. Let us study only the maximum value of this distance:

$$d_{\mathrm{max}}^N = \max_{0 \leq k \leq N} |x_{k+n_0} - x_k| \tag{18}$$

If the attractor is nonsmooth, then d_{max}^N is expected for large enough N to be of the order of the size of the attractor. It is important to note, that for a "true" SNA this behavior does not depend on the initial phase shift ε_0. That means, that the saturated value $d_{\mathrm{max}} \equiv d_{\mathrm{max}}^\infty$ does not depend on ε_0, but the time N to obtain this maximum increases. If the attractor is a smooth one, then the distance of neighboring points on the attractor gets smaller and tends to zero with decreasing phase difference ε_0. In Fig. 12 we present the results of the numerical computations of d_{max} for system (2,3) and different values of ε_0 and α. Again, one can distinguish cases of SNA ($\alpha = 0$) and smooth attractors $\alpha \neq 0$. The number of iterations which is necessary to achieve the saturated maximum distance d_{max} can be estimated as $N \sim \varepsilon_0^{-1}$.

18

5   Conclusions

We have applied the approach of rational approximations to the study of strange non-chaotic attractors in quasiperiodically driven nonlinear systems. It has been shown that such an approximation yields a suitable method to estimate the smoothness properties of an attracting set. The transition from nonstrange to strange attractor then corresponds to the appearance of bifurcations of the attracting set, where the phase shift is considered as a parameter.

Furthermore, we have shown that the SNAs in quasiperiodically forced dynamical systems can be characterized in terms of sensitivity. While chaotic attractors are sensitive to initial conditions, SNAs are sensitive to the perturbations of the phase of the driving force. This sensitivity appears when positive local Lyapunov exponents can be observed for arbitrary long time intervals.

The notion of local Lyapunov exponents was applied previously only to chaotic dynamical systems. Indeed, in chaotic systems there is a rich enough variety of trajectories that may have different Lyapunov exponents (e.g., different periodic orbits typically have different Lyapunov exponents). In non-chaotic systems with periodic behavior, the Lyapunov exponent of the periodic motion is determined uniquely. The point is that in nonchaotic systems with quasiperiodic behavior different trajectories may have different Lyapunov exponents, and a nontrivial distribution of local Lyapunov exponents can be expected as typical. This explains why SNAs are typically observed in quasiperiodically driven systems near the transition to chaos: at the transition point the usual Lyapunov exponent crosses zero, so near the transition point it is natural to expect that the distribution of local Lyapunov exponents will be nonzero for positive exponents. We would also like to mention that the importance of local Lyapunov exponents for SNAs was noticed implicitly in ref.[23], where a method of generating SNA, based on taking pieces of trajectories with positive and negative Lyapunov exponents, was discussed.

Finally, we have proposed an easy test for the occurrence of SNAs in measured time series based on the evaluation of the maximum distance between two trajectories with a given phase shift. But it has to be mentioned that the computation of the maximum distances distinguishes only between strange and nonstrange behavior. It is not useful to make a distinction between strange non-chaotic and chaotic since the maximum distance reaches in both cases the size of the attractor [24].

References

[1] C.Grebogi, E.Ott, S.Pelikan, and J.A.Yorke, Physica D **13**, 261 (1984).

[2] M.Ding, C.Grebogi, and E.Ott, Phys.Rev.A **39**, 2593 (1989).

[3] M.Ding, C.Grebogi, and E.Ott, Phys.Lett.A **137**, 167 (1989).

[4] F.J.Romeiras *et al.*, Physica D **26**, 277 (1987).

[5] T.Kapitaniak, E.Ponce, and J.Wojewoda, J.Phys. A **23**, L383 (1990).

[6] W.L.Ditto *et al.*, Phys. Rev. Letters **65**, 533 (1990).

[7] J.Heagy and W.L.Ditto, J. Nonlinear Science **1**, 423 (1991).

[8] T.Zhou, F.Moss, and A.Bulsara, Phys. Rev. A **45**, 5394 (1992).

[9] F.J.Romeiras and E.Ott, Phys.Rev.A **35**, 4404 (1987).

[10] A.Bondeson, E.Ott, and T.M.Antonsen, Phys.Rev.Lett **55**, 2103 (1985).

[11] H. G. Schuster, *Deterministic Chaos, An Introduction* (VCH – Verlag, Weinheim, 1988).

[12] A. J. Lichtenberg and M. A. Lieberman, *Regular and Chaotic Dynamics* (Springer, New York, 1992).

[13] J.F.Heagy and S.M.Hammel, Physica D **70**, 140 (1994).

[14] J.M.Greene, J. Math. Phys. **20**, 760 (1979).

[15] R.S.MacKay, Physica D **7**, 283 (1983).

[16] M.J.Feigenbaum, L.P.Kadanoff, and S.J.Shenker, Physica D **5**, 370 (1982).

[17] D.Rand, S.Ostlund, J.Sethna, and E.D.Siggia, Phys.Rev.Lett **49**, 132 (1982).

[18] P.Grassberger, in *Chaos*, edited by A.V.Holden (Manchester University Press, Manchester, 1986).

[19] P.Grassberger, R.Badii, and A.Politi, J. Stat. Phys. **51**, 135 (1988).

[20] H.D.I.Abarbanel, R.Brown, and M.B.Kennel, J. Nonlinear Sci. **2**, 343 (1992).

[21] H.Fujisaka, Prog.Theor.Phys. **70**, 1264 (1983).

[22] J.-P. Eckmann and I. Procaccia, Phys. Rev. A **34**, 659 (1986).

[23] T.Kapitaniak, Phys. Rev. E **47**, 1408 (1993).

[24] C.Nicolis and G.Nicolis, Phys. Rev. A **43**, 5720 (1991).